Underwater Signal Detection in Partially known Ocean using Short Acoustic Vector Sensor Array

V.N. Hari[1], G.V. Anand[2], A.B. Premkumar[1], A.S. Madhukumar[1]

[1] School of Computer Engineering, Nanyang Technological University, Singapore 639798, phone: + (65)98124684

[2]Department of Electrical Communication Engineering, Indian Institute of Science, Bangalore 560012, India, phone: + (91)80-22932277

Abstract: **A new narrowband signal detection method called subspace detection (SD) [1] was proposed recently for achieving improved detection performance in shallow ocean. The SD method requires the knowledge of mode functions and modal wavenumbers of the ocean channel. In this paper we present three new methods of narrowband signal detection in a partially known ocean using an array of acoustic vector sensors (AVS). These methods require less prior information about the ocean channel; and yet they provide a better performance than SD especially at higher signal frequencies or shorter array lengths. Two of the new methods require only knowledge of sound speed at the sensor locations. The performance of the proposed methods is frequency-independent. These methods can be used with arrays in either horizontal or vertical configurations, and with either linear or circular geometries.**

Index Terms—*vector sensors, detection, array processing, shallow ocean*

I. INTRODUCTION

The use of acoustic vector sensors (AVS) for source localization and tracking is gaining popularity due to their numerous proven advantages over traditional acoustic pressure sensors (APS) or hydrophones [2]. In addition to measuring the acoustic pressure, an AVS also measures the particle velocity at a point in space. This provides a better characterization of the acoustic field at the point of measurement as compared to the APS. The additional information given by the velocity measurements has been shown to yield improved estimates over the APS in source localization and tracking problems. Another advantage of AVS arrays is that they do not manifest either the steering vector ambiguity associated with spatial undersampling or the left-right ambiguity [2],[3]. These advantages have spurred the development of a large number of algorithms and methods based on AVS. After their applicability and use was demonstrated theoretically and experimentally by D'Spain et al [4],[5] and some early theoretical work by Nehorai and Paldi [2], numerous advances have been made in improved localization and tracking and several methods employing AVS have been developed.

However, no attention has been given to the problem of signal detection using AVS apart from the work done by Krishna and Anand [1]. They have presented a method called subspace detection (SD) method for narrowband signal detection in shallow ocean. They also present the so-called unconstrained detector (UD) derived using the conventional approach to detection based on GLRT [6]. The UD, which uses no prior information about the ocean channel other than the sound speed at the elements of the sensor array, is similar to an energy detector in the case of an APS array. The subspace detector SD utilizes the fact that the array signal vector belongs to the space spanned by the eigenfunctions (normal mode functions) of the channel. Consider an APS array of N sensors, and let M be the number of normal modes. If $M < N$, the N-dimensional signal vector belongs to a lower (M) dimensional subspace, which may be called the signal subspace. Assuming that the mode functions are known, the SD exploits the knowledge of the signal subspace to obtain a performance which is superior to that of the UD which does not utilize this knowledge.

The SD has a few limitations. As the signal frequency is increased, the number of normal modes M also increases. For a fixed array length N, increase in the dimension of the signal subspace M causes a corresponding reduction in the dimension of the noise subspace $N - M$, and a consequent degradation in the performance of the SD. If M is greater than or equal to N, the SD reduces to UD. Another limitation of the SD is that it requires knowledge of the modal wave numbers and eigenfunctions of the ocean channel. If this information is not available the SD method becomes inapplicable, and modeling errors lead to degradation in the performance of SD.

This paper presents three novel methods of detection using AVS, namely the Approximate Signal vector Form Detector (ASFD), Truncated Signal vector Form Detector (TSFD), and Truncated Subspace Detector (TSD). The ASFD and the TSFD require no ocean channel information other than the sound speed at the location of the sensor array elements. Usually, this information can be easily obtained. These two methods use the relationship among the acoustic pressure and particle velocity components of the signal at each sensor. The TSD is a modified version of the SD that uses a truncated normal mode model (smaller number of modes) for detection. The performance of the proposed methods is frequency-independent, and all of them outperform the SD at higher frequencies or for shorter array lengths.

The paper is structured as follows. Section II presents the data model. Section III presents a review of the subspace detection method and Section IV presents the formulation of the new detection methods. Section V presents simulation results to demonstrate the superior performance of the proposed methods, and Section VI concludes the paper.

II. DATA MODEL

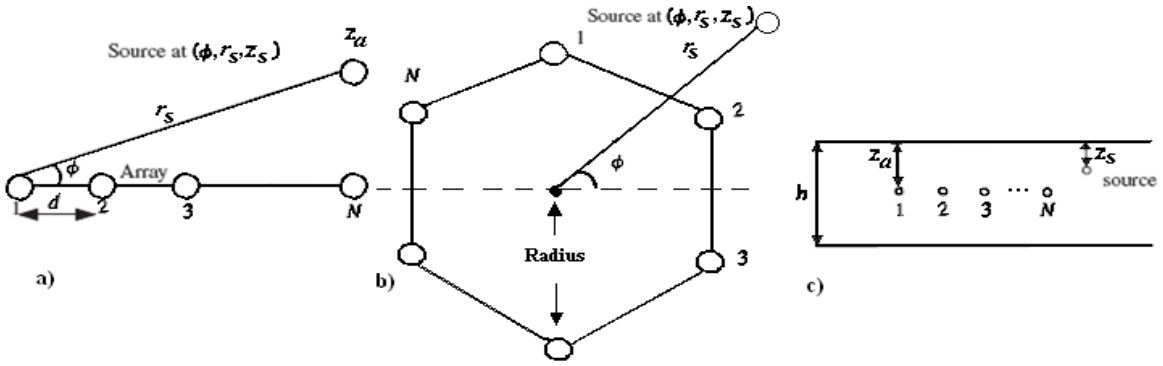

Fig. 1: Geometry of the source and receiver array, (a) top view of HLA (b) top view of HCA, (c) side view for horizontal arrays

Consider the problem of detection of a narrowband point source with center frequency f located in a range – independent shallow ocean at a depth z_s and range r_s with respect to an N–element AVS array. The n^{th} AVS in the array has three outputs – acoustic pressure and two orthogonal horizontal components of particle velocity. The z component of velocity is not considered for detection in this paper. The source azimuth angle ϕ is measured with respect to a horizontal axis through the reference point of the array which is located at a depth z_a. The sensor array is assumed to be in the far-field region with respect to the source. We consider three array configurations, namely the horizontal linear (HLA), horizontal circular (HCA) and vertical linear (VLA) array configurations. The sensors are uniformly spaced within the linear arrays, and the first sensor is considered to be the reference point (topmost sensor in the case of VLA). The elements of the HCA are at the vertices of a regular polygon with N – sides, and the reference point is the center of the array. The top view of the geometry of the HLA and HCA are shown in Figs. 1 (a) and (b) respectively, and the side view is shown in Fig. 1 (c).

Let $\boldsymbol{x}$, $\boldsymbol{s}$ and $\boldsymbol{w}$ denote, respectively, the $3N$ x 1 data vector, signal vector and noise vector respectively at the AVS array. The vector $\boldsymbol{s}$ can be expressed as

$$\boldsymbol{s} = [\boldsymbol{s}_1{}^{\mathrm{T}} \boldsymbol{s}_2{}^{\mathrm{T}} \ldots \boldsymbol{s}_N{}^{\mathrm{T}}]^{\mathrm{T}}, \tag{1}$$

where

$$\boldsymbol{s}_n = [p_n v_{xn} v_{yn}]^{\mathrm{T}}. \tag{2}$$

denotes the signal vector at the n^{th} sensor of an N-sensor located at coordinates (x_n, y_n) with respect to the reference point of the array. In (2), p_n denotes the complex amplitude of acoustic pressure, and (v_{xn}, v_{yn}) denote complex amplitudes of the horizontal (x, y) components of particle velocity. According to the normal mode propagation model, the pressure p_n can be approximated by a sum of M discrete normal modes given by [3]

$$p_n = \sum_{m=1}^{M} p_{mn} = \boldsymbol{u}^{\mathrm{T}} \boldsymbol{a}_n, \tag{3}$$

where

$$\boldsymbol{u} = [\,1\ 1 \ldots 1\ (M \text{ times})]^{\mathrm{T}}, \tag{4}$$

$$\boldsymbol{a}_{\mathrm{n}} = [p_{1\mathrm{n}} p_{2\mathrm{n}} \ldots \ p_{M\mathrm{n}}]^{\mathrm{T}}, \tag{5}$$

and p_{mn} refers to the contribution of the m^{th} mode to the pressure measurement at the n^{th} sensor, given by

$$p_{mn} = B_0\, \psi_m(z_n)\, \psi_m(z_s)\, g_m(r_s) \Omega(\phi) \tag{6}$$

where z_n is the depth of the n^{th} sensor, ψ_m is the normalized eigen function of the m^{th} normal mode, k_m is the corresponding modal wave number (real part of the eigen value), B_0 is a complex quantity independent of r_s, z_s and z_n which determines the strength of the source, and g_m is given by

$$g_m(r_s) = e^{ik_m r_s} / \sqrt{k_m r_s}\ . \tag{7}$$

The phase term $\Omega(\phi)$ is unity for vertical arrays, and for horizontal arrays it is given by the expression

$$\Omega(\phi) = e^{ik_m (x_n Cos(\phi) + y_n Sin(\phi))}\ . \tag{8}$$

For a given channel, the number of propagating modes M depends on the signal frequency. In general, M increases as the frequency is increased.

Using (3) and (6) along with the law of conservation of momentum, and invoking the far-field approximation ($k_m r_s >> 1$), the complex amplitudes of x and y components of the particle velocity at the n^{th} sensor can be found. For the sake of homogeneity, the velocity components are scaled by the factor $\sqrt{2}\,\rho c(z)$, where ρ denotes the density of water and $c(z)$ is the speed of sound at the depth z. The expressions for the scaled velocity components are given by [3]

$$v_{xn} = \cos(\phi) \sum_{m=1}^{M} d_m p_{mn} = \cos(\phi) \boldsymbol{d}^{\mathrm{T}} \boldsymbol{a}_{\mathrm{n}}\ , \tag{9}$$

$$v_{yn} = \sin(\phi) \sum_{m=1}^{M} d_m p_{mn} = \sin(\phi) \boldsymbol{d}^{\mathrm{T}} \boldsymbol{a}_{\mathrm{n}}, \tag{10}$$

where

$$\boldsymbol{d} = [d_1\, d_2 \ldots .\ d_{\mathrm{M}}]^{\mathrm{T}}, \tag{11}$$

and d_m is given by

$$d_m = \sqrt{2}\, k_m / k(z), \tag{12}$$

where

$$k(z) = c(z)/(2\pi f). \tag{13}$$

It is assumed that the signal at the AVS array is embedded in additive white Gaussian noise. We may also assume the noise to be spatially white in the horizontal direction. But the noise is spatially non – stationary in the vertical direction. For two sensors at depths z_i and z_j in the Pekeris channel, the correlation assumes the form [3]

$$\mathbf{R}(z_i, z_j) = \sigma^2 r(z_i, z_j)\mathbf{I}_3 \tag{14}$$

where $\mathbf{I}_3$ is the 3x3 identity matrix, $r(z_i, z_j)$ is defined as

$$r(z_{i,} z_j) = \frac{\sum_{m=1}^{M} sin(m\gamma z_i) sin(m\gamma z_j)}{\sum_{m=1}^{M} sin^2(m\gamma z_1)} = r(z_j, z_i) \tag{15}$$

and the parameter σ^2 is a measure of noise intensity. The correlation matrix of the array noise vector $\boldsymbol{w}$ can be written as

$$\mathbf{R}_w = \sigma^2 \mathbf{R}_0 \tag{16}$$

The matrix $\mathbf{R}_0$ is defined as

$$\mathbf{R}_{0,hor} = r(z_{a,} z_a)\, \mathbf{I}_{3N} \tag{17}$$

for a horizontal array at depth z_a, and as

$$\mathbf{R}_{0,ver} = \begin{bmatrix} \mathbf{R}(z_1, z_1) & \mathbf{R}(z_1, z_2) & ..... & \mathbf{R}(z_1, z_N) \\ . & & & \\ . & & & \\ \mathbf{R}(z_N, z_1) & ..... & & \mathbf{R}(z_N, z_N) \end{bmatrix}. \tag{18}$$

for a vertical array.

III. Review of Subspace Detection

A major source of difficulty in signal detection in a shallow ocean is that the signal vector $\boldsymbol{s}$ at the sensor array depends on the location of the source which is unknown. One may perform a generalized likelihood ratio test (GLRT) by treating $\boldsymbol{s}$ as an unknown vector and maximizing the likelihood ratio with respect to $\boldsymbol{s}$. This procedure leads to an energy detector. However, a better alternative is available if $3N > M$, where N is the number of sensors in the AVS array and M is the number of normal modes. In this case, the $3N$ dimensional AVS array signal vector belongs to a lower (M) dimensional subspace. The subspace detector (SD) exploits this prior information by maximizing the likelihood ratio with respect to $\boldsymbol{s}$ under the constraint that $\boldsymbol{s}$ belongs to a known M dimensional subspace. The energy detector, which is obtained by performing an unconstrained optimization of the likelihood ratio, will be referred to as the unconstrained detector (UD).

The detection problem can be cast in the form of the following hypothesis testing problem:

$$\begin{aligned} &H_0 : \boldsymbol{x} = \boldsymbol{w} \\ &H_1 : \boldsymbol{x} = \boldsymbol{s} + \boldsymbol{w}, \end{aligned} \tag{19}$$

It is seen from (1) – (13) that the signal vector $\boldsymbol{s}$ can be expressed as

$$\boldsymbol{s} = \mathbf{H}\, \boldsymbol{q}\ , \tag{20}$$

where

$$\boldsymbol{q} = [q_1 \ldots q_M]^T\ , \tag{21}$$

$$q_m = B_0\, g_m(r_s)\, \psi_m(z_s);\ m = 1,.., M. \tag{22}$$

In (20), $\mathbf{H}$ is a $3N$ x M matrix with linearly independent columns if $3N \geq M$. Explicit expressions for the elements of $\mathbf{H}$ are given in [1]. It follows that the $3N$ x 1 signal vector $\boldsymbol{s}$ belongs to the M – dimensional subspace spanned by the columns of $\mathbf{H}$ if $3N > M$. But the structure of the vector $\boldsymbol{s}$ is not suitable for the application of the SD algorithm [1]. In order to modify the structure of the signal vector, we consider the singular value decomposition of $\mathbf{H}$:

$$\mathbf{H} = \mathbf{U}\, \mathbf{D}\, \mathbf{V}^H\ , \tag{23}$$

where $\mathbf{U}$ is a $3N$ x $3N$ unitary matrix. The unitary transformation

$$\tilde{\ } \tag{24}$$

converts the array signal vector to the form

$$\tilde{\ } \quad \tilde{\ } \quad]^T\ , \tag{25}$$

where $\tilde{\ }$ is a vector of dimension M and $\mathbf{0}_{3N-M}$ is a zero vector of dimension $3N - M$. The structure of the transformed vector $\tilde{\ }$ is amenable to the application of the SD algorithm. By applying this transformation to the data vector and the noise vector, we get

$$\tilde{\ } \tag{26}$$

$$\tilde{\ } \tag{27}$$

The correlation matrix of the transformed noise vector $\tilde{\ }$ is given by

$$\mathbf{R}_{\tilde{\ }} \quad ^2]\tilde{\ } \quad \tilde{\ } \quad {}_0\mathbf{U}. \tag{28}$$

The detection problem is (19) can now be recast as

$H_0 : \tilde{\ } \quad \tilde{\ }$

$$H_1 : \tilde{} \quad \tilde{} \quad \tilde{} \tag{29}$$

We shall consider the detection problem for two different cases:

(a) the noise intensity parameter σ^2 is known, and

(b) σ^2 is unknown.

The correlation matrix $\mathbf{R}_0$ defined in (17) or (18) is always assumed to be known. Lack of knowledge of σ^2 leads to a degradation of performance. This degradation can be arrested if the data vector $\boldsymbol{x}$ is augmented by a set of K independent and identically distributed (i.i.d) secondary data vectors (sdv) $\{\boldsymbol{z}(j); j = 1, ...,K;\ K \geq N\}$. These secondary data vectors are statistically independent of the primary data vector $\boldsymbol{x}$ and have the same distribution as the noise $\boldsymbol{w}$. The transformed version of the secondary data vectors may be denoted as

$$\tilde{}(j) = \mathbf{U}^{\mathrm{H}} \boldsymbol{z}(j); j = 1, . ., K. \tag{30}$$

The joint likelihood functions of the transformed primary and secondary data vectors under hypotheses H_0 and H_1 are given by

$$f\left(\tilde{} \ \tilde{} \quad \tilde{} \quad H_0\right) = \frac{1}{\left(\pi^{3N} |\sigma^2 \tilde{}\right.} \quad \text{p}\left[-\frac{1}{\sigma^2}\left[\tilde{} \quad \tilde{} \right.\right. \tag{31}$$

$$f\left(\tilde{} \ \tilde{} \quad \tilde{} \quad \tilde{} \right. = \frac{1}{\left(\pi^{3N} |\sigma^2 \tilde{}\right.} \quad \text{p}\left[-\frac{1}{\sigma^2}\left[\left(\tilde{} \quad \tilde{} \quad \tilde{} \right.\right.\right. \tag{32}$$

where

$$\sigma_K^2 = \sum_{j=1}^{K} \tilde{} \quad \tilde{} \quad \left(j\right) \mathbf{R}_0^{-1} \boldsymbol{z}(j). \tag{33}$$

If σ^2 is unknown (case (b)), maximization of the likelihood functions with respect to σ^2 gives

$$f\left(\tilde{} \ \tilde{} \quad \tilde{} \right. = \left. \frac{1}{\left[\left(\pi e\right)^{3N} \right.} \right. \tag{34}$$

$$f\left(\tilde{} \ \tilde{} \quad \tilde{} \right. \left. \frac{1}{\left(\pi e\right)^{} \right.} \tag{35}$$

where

$$\left. \frac{1}{3N(K+1)}\left[\tilde{} \quad \tilde{} \right.\right. \tag{36}$$

$$\left. \frac{1}{3N(K+1)}\left[\left(\tilde{} \quad \tilde{} \right.\right.\right. \tag{37}$$

In the case of the unconstrained detector (UD), the signal vector $\boldsymbol{s}$ is considered to be completely unknown. The likelihood function in (32) is maximized with respect to $\tilde{}$ if we choose the estimate $\tilde{} \quad \tilde{}$. Hence the generalized likelihood ratio (GLR) for the UD in the case (a) (σ^2 is known), is obtained by taking the ratio of the expressions in (32) and (31), with $\tilde{} \quad \tilde{}$. The corresponding test statistic of the UD is given by

$$\gamma_{UD} = \tilde{} \quad \tilde{} \quad \mathfrak{c}, \tag{38}$$

In case (b) (σ^2 is unknown), the UD does not provide any meaningful solution.

Let the transformed vectors $\tilde{}$ and $\tilde{}$ be partitioned as

$$\tilde{} \quad \tilde{} \quad \tilde{} \quad \tilde{} \quad \tilde{} \quad \left.\right]^T, \tag{39}$$

where $\tilde{}$ and $\tilde{}$ are vectors of dimension M and $\tilde{}$ and $\mathbf{0}_{3N-M}$ are vectors of dimension $3N - M$. Let $\tilde{}$ be partitioned as

$$\tilde{} \quad \left[\begin{array}{cc} \tilde{} & \tilde{} \\ \tilde{} & \tilde{} \end{array}\right. \tag{40}$$

where $\tilde{}$ and $\tilde{}$ are square matrices of size M x M and ($3N$-M) x ($3N$-M) respectively. It can be shown that

$$\tilde{}^{\mathrm{H}} \tilde{}_0^{-1} \tilde{} = \tilde{}_2^{\mathrm{H}} \tilde{}_{22}^{-1} \tilde{}_2 + \tilde{}_{1,2}^{\mathrm{H}} \tilde{}_{1,2}^{-1} \tilde{}_{1,2}, \tag{41}$$

$$(\tilde{} - \tilde{})^{\mathrm{H}} \tilde{}_0^{-1} (\tilde{} - \tilde{}) = \tilde{}_2^{\mathrm{H}} \tilde{}_{22}^{-1} \tilde{}_2 + (\tilde{}_{1,2} - \tilde{})^{\mathrm{H}} \tilde{}_{1,2}^{-1} (\tilde{}_{1,2} - \tilde{}), \tag{42}$$

where

$$\tilde{}_{1,2} = \tilde{}_1 - \tilde{}_{12} \tilde{}_{22}^{-1} \tilde{}_2, \tag{43}$$

$$\tilde{}_{1,2} = \tilde{}_{11} - \tilde{}_{12} \tilde{}_{22}^{-1} \tilde{}_{21}. \tag{44}$$

On combining (32) and (42) it is seen that the likelihood function in (32) is maximized when $\tilde{}$ is estimated as $\tilde{} = \tilde{}_{1,2}$. On performing maximization in this fashion, taking the ratio of the likelihood functions in (32) and (31), and using (41) and (42), we get the GLR of the subspace detector. Further simplification leads to the following test statistic

$$\gamma_{SD,Case\ (a)} = \tilde{}_{1,2}^{\ H} \tilde{}_{1,2}^{-1} \tilde{}_{1,2}, \tag{45}$$

$$\gamma_{SD,Case\ (b)} = \tilde{} \quad \tilde{} \quad \tilde{} \quad \tilde{} \tag{46}$$

IV. Formulation of New Detectors

A. Truncated Subspace detector (TSD)

The SD outperforms the UD because the former uses the fact that the $3N$ - dimensional signal vector belongs to a lower (M) dimensional subspace. But for a given N, the performance of SD degrades as the signal frequency is increased because an increase in frequency leads to an increase in M and a corresponding reduction in the dimension $3N - M$ of the noise subspace.

In order to arrest this degradation, we propose a detector which limits the number of modes of the signal used for detection to T, where $T < M$. This detector, which uses a truncated signal model, is referred to as the TSD. This truncation causes a degradation of the signal model, but it increases the dimension of the noise subspace for a given array length N, and also reduces the computational complexity involved in detection. The benefit of increased dimension of the noise subspace dominates the error due to inferior signal modeling, especially at higher frequencies. Hence the TSD is seen to outperform the SD.

In the case of TSD, $\tilde{\Gamma}$ is a (T by T) square matrix consisting of the first T rows and columns of $\tilde{\Gamma}$, $\tilde{\Gamma}$ is a ($3N$-T) by ($3N$-T) square matrix, and $\tilde{\Gamma}$ and $\tilde{\Gamma}$ constitute the remaining blocks of $\tilde{\Gamma}$. The test statistics for the TSD are derived in the same way as the SD, and have the same form as that of the SD in (45) and (46).

B.Truncated Signal vector Form detector (TSFD)

The TSFD which is also based on the GLRT uses a different approach for estimating the unknown signal vector $\boldsymbol{s}$. Now the detection problem is expressed as in (19), and the transformations defined in (26), (27) and (30) are not used. From (2), (3), (9) and (10), estimation of $\boldsymbol{s}$ involves the estimation of the unknown vectors $\boldsymbol{d}$ and $\boldsymbol{a}_n$, n = 1, 2… N. In order to find these estimates, we equate the derivatives of the likelihood function under hypothesis H_1 ((32) with all transformed vectors replaced by their untransformed versions) with respect to $\boldsymbol{a}_n$ and $\boldsymbol{d}$ to zero to obtain the following equations

$$\mathbf{T}_{\mathrm{d}}\,[\,\mathrm{Re}(\boldsymbol{a}_{\mathrm{n}})\;\;\mathrm{Im}(\boldsymbol{a}_{\mathrm{n}})] = [\,\mathrm{Re}(\boldsymbol{y}_{\mathrm{d}})\;\;\mathrm{Im}(\boldsymbol{y}_{\mathrm{d}})\,],\quad n = 1, \ldots, N, \tag{47}$$

$$\mathbf{T}_{\mathrm{p}}\boldsymbol{d} = \boldsymbol{y}_{\mathrm{p}}\,, \tag{48}$$

where Re($\boldsymbol{x}$) and Im($\boldsymbol{x}$) indicate vectors formed from the real and imaginary parts of vector $\boldsymbol{x}$ respectively, and $\boldsymbol{y}_{\mathrm{d}}$ and $\boldsymbol{y}_{\mathrm{p}}$ are M by 1 vectors defined as

$$\boldsymbol{y}_{\mathrm{d}} = [x_{\mathrm{n1}} + z_{\mathrm{n}}.d_1 \ldots x_{\mathrm{n1}} + z_{\mathrm{n}}.d_{\mathrm{M}}]^{\mathrm{T}}, \tag{49}$$

$$\boldsymbol{y}_p = [\sum_{n=1}^{N}[\mathrm{Re}(z_n)\,\mathrm{Re}(p_{1n}) + \mathrm{Im}(z_n)\,\mathrm{Im}(p_{1n})] \ldots \sum_{n=1}^{N}[\mathrm{Re}(z_n)\,\mathrm{Re}(p_{Mn}) + \mathrm{Im}(z_n)\,\mathrm{Im}(p_{Mn})]]^T, \tag{50}$$

where

$$z_{\mathrm{n}} = x_{\mathrm{n2}}\cos(\phi) + x_{\mathrm{n3}}\sin(\phi)\,, \tag{51}$$

$$\mathbf{T}_{\mathrm{d}} = \boldsymbol{u}\boldsymbol{u}^{\mathrm{T}} + \boldsymbol{d}\boldsymbol{d}^{\mathrm{T}}, \tag{52}$$

$$\boldsymbol{T}_p = \sum_{n=1}^{N}\left(\mathrm{Re}(\boldsymbol{a}_n)\,\mathrm{Re}\left(\boldsymbol{a}_n^T\right) + \mathrm{Im}(\boldsymbol{a}_n)\,\mathrm{Im}\left(\boldsymbol{a}_n^T\right)\right) \tag{53}$$

and $\boldsymbol{u}$ is defined in (4). It is known that

$$\sqrt{2} > d_1 > d_2 > \ldots d_{\mathrm{M}} > \sqrt{2}\,c(h)\,/\,c_{\mathrm{b}}, \tag{54}$$

where h is the depth of the ocean, and c_b is the speed of sound in the sediment. This bound can be used to make an initial estimate of $\boldsymbol{d}$. Hence, the algorithm to find the maximum likelihood estimate (MLE) $\hat{\ }_n$ of $\boldsymbol{s}_n$ is as follows. For each ϕ, use the initial estimate of $\boldsymbol{d}$ to solve equations (47) and (48) iteratively to obtain the estimates of $\boldsymbol{d}$ and $\boldsymbol{a}_n$. For M> 2, these form an under - determined system of equations, hence it is required to use the minimum norm solution of (47) and (48). Two iterations are found to be sufficient since the initial estimate of $\boldsymbol{d}$ is quite good due to the bounds provided by the inequalities in (54). Thus we obtain the estimate $\hat{\ }_n$ that maximizes the likelihood function under H_1 for case (a) or (b). Finally, this likelihood function is maximized with respect to the unknown ϕ.

The test statistic for the TSFD is obtained by considering a ratio of the likelihood functions under H_1 and H_0 respectively, maximized with respect to all unknown parameters. For the cases (a) and (b), the test statistics are

$$\gamma_{TSFD,Case\,(a)} = \max_{\phi}\left[\sum_{n=1}^{N}\left[2\mathrm{Re}\left(\boldsymbol{x}_n^H\mathbf{R}_0^{-1}\hat{\ }_n\right),\quad \hat{\ }_n\quad \hat{\ }_n\right]\right] \tag{55}$$

and

$$\gamma_{TSFD,Case\,(b)} = \frac{\boldsymbol{x}_n^H\mathrm{R}_0^{-1}\boldsymbol{x}_n + \sigma_K^2}{\boldsymbol{x}_n^H\mathrm{R}_0^{-1}\boldsymbol{x}_n - \gamma_{TSFD,Case\,(a)} + \sigma_K^2} \tag{56}$$

respectively, where $\hat{\ }_n$ is found by the method outlined above using equations (2),(3),(9),(10), (47) and (48).

Since this iterative method involves estimation of a large number of unknowns ($\boldsymbol{d}$ and $\boldsymbol{a}_{\mathrm{n}}$, n = 1, 2… N) using fewer equations, the method may sometimes be ineffective due to inaccuracy in estimation of the unknowns. The computational burden also increases as the number of iterations is increased. Hence, in order to reduce the computational burden and increase accuracy, it is necessary to truncate the number of modes used to T modes, where $T < M$. Since most of the signal energy resides in a small number of lower order modes, discarding the higher order modes introduces a relatively small error in the signal model, and this error is overridden by the improvement in the estimates of $\boldsymbol{d}$ and $\boldsymbol{a}_n$. Hence the detector described in this section with a truncated signal model is designated as the truncated signal vector form detector (TSFD).

C. Approximate Signal vector Form detector (ASFD)

In (11), d_m can be considered very close to $\sqrt{2}$ as $k(z) \sim k_m$. This is a reasonable approximation in view of the tight bounds given in (54). This considerably simplifies the detection problem, and leads to a much simpler detection algorithm which we refer to as the ASFD. The expressions for the (scaled) x and y velocity terms at the n^{th} sensor reduce to

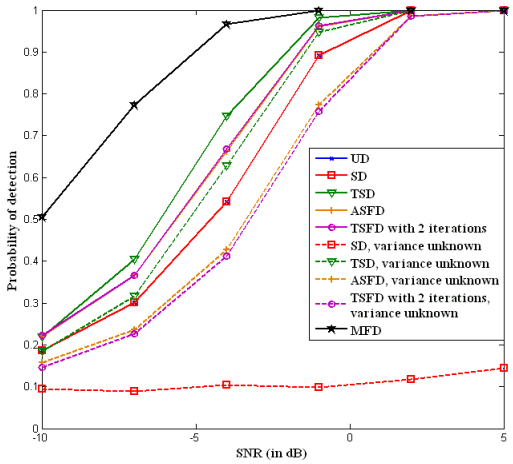

Fig. 2: P_D vs. SNR at P_{FA} = 0.1, f = 380 Hz, array geometry: HLA, source bearing: 33°, no secondary data vectors used

$$\boldsymbol{v}_{xn} = \sqrt{2}\cos(\phi)\boldsymbol{a}_n\,, \tag{57}$$

$$\boldsymbol{v}_{yn} = \sqrt{2}\sin(\phi)\boldsymbol{a}_n\,. \tag{58}$$

We can now express $\boldsymbol{s}_n$ in a simpler form as

$$\boldsymbol{s}_n = p_n \boldsymbol{g}(\phi)\,,\ n = 1, 2\ldots N, \tag{59}$$

where the approximate signal vector (ASFV) $\boldsymbol{g}(\phi)$ is given by

$$\boldsymbol{g}(\phi) = [\,1\ \sqrt{2}\cos(\phi)\ \sqrt{2}\sin(\phi)\,]^{\mathrm{T}}. \tag{60}$$

Hence, the ML estimate of $\boldsymbol{s}$ is achieved by maximizing the likelihood function under hypothesis H_1 with respect to $\{\boldsymbol{p}_n;\ n = 1, \ldots, N\}$. It can be shown that the ML estimate of $\boldsymbol{p} = [\,\boldsymbol{p}_1 \ldots \boldsymbol{p}_N\,]^{\mathrm{T}}$ is given by

$$\hat{\boldsymbol{p}} = \left[\boldsymbol{g}^T(\phi)\boldsymbol{y}_1 \ \ldots \boldsymbol{g}^T(\phi)\boldsymbol{y}_N\right]^T, \tag{61}$$

where

$$\boldsymbol{y}_n = \sum_{j=1}^{K} r^{-1/2}(z_n, z_j)\boldsymbol{x}_j \tag{62}$$

and $\mathbf{W}$ is an N x N matrix whose $(i,j)^{\text{th}}$ element is given by

$$[\mathbf{W}]_{ij} = r^{-1/2}(z_i, z_j). \tag{63}$$

The GLR of the ASFD, conditional to ϕ, may now be obtained by substituting $\boldsymbol{p} = \hat{\boldsymbol{p}}$; and the test statistic of the ASFD may be obtained by maximizing the GLR with respect to ϕ. Thus we obtain the test statistics for cases (a) and (b) to be

$$\gamma_{ASFD,Case\ (a)} = \max_{\phi}\left[\sum_{n=1}^{N}\frac{\left|\boldsymbol{g}^T(\phi)\boldsymbol{y}_n\right|^2}{\boldsymbol{g}^T(\phi)\boldsymbol{g}(\phi)}\right] \tag{64}$$

and

$$\gamma_{ASFD,Case\ (b)} = \frac{\boldsymbol{x}^H\mathbf{R}_0^{-1}\boldsymbol{x} + \sigma_K^2}{\boldsymbol{x}^H\mathbf{R}_0^{-1}\boldsymbol{x} - \gamma_{ASFD,Case\ (a)} + \sigma_K^2} \tag{65}$$

respectively. This detector is called the approximate signal vector form detector (ASFD) since it is based on an approximate determination of the AVS signal vector.

D. Matched filter detector (MFD)

Apart from the above mentioned detectors, we also consider another detector, namely the MFD. The MFD is the optimal detector in Gaussian environmental noise when full information regarding the signal source $\boldsymbol{s}$ is available. Thus, it may be used as a benchmark against which other detection methods may be compared. However, it should be noted that the matched filter is an unrealizable detector since the position of the source is not known, and hence the signal vector itself cannot be known. The MFD has a test statistic given by

$$\gamma_{MFD} = \mathrm{Re}(\boldsymbol{x}^{\mathrm{H}}\mathbf{R}_0^{-1}\boldsymbol{s}). \tag{66}$$

where Re(.) denotes real part of. It may also be noted that, in the conventional sense, the matched filter or correlation detector refers to a detector which performs correlation in the time domain. However, in the present context, the correlation of the pre-whitened observation vector $\tilde{\boldsymbol{x}}$ and the pre-whitened signal vector $\tilde{\boldsymbol{s}}$ is performed in the spatial domain.

V. Simulation Results

Simulation results are presented in this section to compare the performance of the three new detectors TSD, TSFD and ASFD with those of the existing detectors SD, UD and the unrealizable optimal detector MFD. The ocean is modeled as a Pekeris channel comprising a homogeneous water layer of constant depth over a fluid half – space. The following values of channel, source and array parameters have been assumed: sound speed in water c =1500 m/s, density of water ρ = 1000 kg/m^3, water column depth = 70m, sound speed in ocean bottom c_b = 1700 m/s, density of ocean bottom ρ_b = 1500 kg/m^3, source range r_s = 5000 m, source depth z_s = 40 m, bearing $\phi = 33^0$, source frequency f = 380 Hz unless otherwise stated, number of sensors (in the array) N = 6, distance between adjacent sensors = 9.6 m, depth of HLA/HCA = 40 m, depth of topmost element of VLA = 15 m. For the above mentioned choice of parameters, the number of modes in the channel is M = 17 .The signal-to-noise ratio (SNR) at the array is defined as

$$SNR_{array} = \frac{1}{N}\sum_{n=1}^{N}(SNR)_n\,, \tag{67}$$

where

$$(SNR)_n = |p_n|^2/\sigma_n^2 \tag{68}$$

is the SNR at the n^{th} sensor, and σ_n^2 is the variance of the noise at the pressure measurement of the n^{th} sensor.

Figure 2 shows plots of probability of detection P_D versus SNR for probability of false alarm P_{FA} = 0.1. The TSD and TSFD have been implemented using only the first normal mode, i.e, T = 1, and two iterations have been used in TSFD

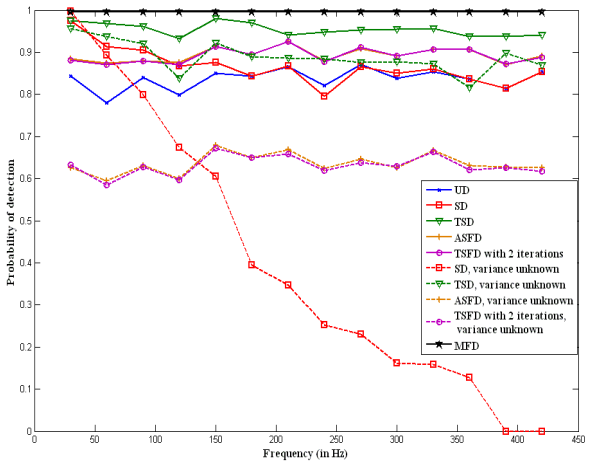

Fig. 3: P_D vs. signal frequency at $P_{FA} = 0.1$, SNR = -2 dB, array geometry: HLA, source bearing: 33°, no secondary data vectors

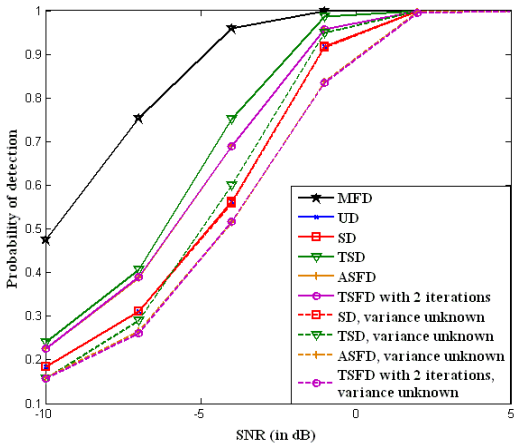

Fig. 4: P_D vs. SNR at $P_{FA} = 0.1$, $f = 380$ Hz, array geometry: HLA, source bearing: 33°, 5 secondary data vectors used

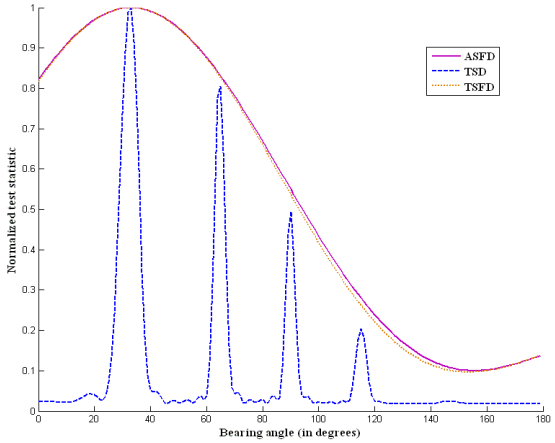

Fig. 5: Normalized test statistic vs. bearing angle, SNR = -2 dB, $f = 380$ Hz, array geometry: HLA, source bearing: 33°

for estimating $\boldsymbol{d}$ and $\{\boldsymbol{a}_n;\ n = 1,\ldots N\}$. No secondary data vectors have been used for implementing SD, TSD, TSFD and ASFD for the case of unknown σ^2. The plots in Fig. 2 indicate that the new detectors presented in this work outperform the existing methods of detection at the signal frequency considered. The MFD, which is assumed to have full information about the signal vector, has the best performance among all the detectors considered. However, among the realizable detectors under consideration, the TSD (with $T = 1$) performs the best. The ASFD and TSFD (with $T = 1$) are seen to be almost equal in performance. This shows that the approximation $k_m \sim k(z)$ does not lead to appreciable deterioration in performance of the ASFD and is therefore justified. The ASFD is also less complex to implement than TSFD as can be seen from the analysis presented in section IV. Both these methods perform better than the UD and SD at the frequency considered.

The unavailability of knowledge of the noise variance σ^2 is expected to lead to deterioration of performance of the detectors and this is reflected in Fig. 2. However, the performance of the TSD does not degrade considerably even if the variance σ^2 is unknown, since it has noise subspace of large dimension to compensate for lack of knowledge of noise. The performance of the SD, on the other hand, is seen to degrade considerably if σ^2 is unknown. This is because at the high frequency considered, the SD has a noise subspace of very low dimension which can provide very little information about the noise.

The variation of the P_D of the detectors with variation in the frequency of the signal source is shown in Fig. 3. The TSD is seen to yield the best performance among all the realizable detectors at all frequencies of the signal and its performance is also close to that of the optimal but unrealizable MFD. The ASFD and TSFD both perform better than the UD at all frequencies and also better than the SD at high frequencies. It is noteworthy that the performance of SD degrades with increasing frequency for a given array size, whereas the performances of the other detectors are largely independent of frequency. The reason for the deterioration in performance of the SD has been explained in [1]. This is because the noise subspace reduces in dimension as the number of modes increases, and hence the SD has less information about the noise. Subsequently, at a certain value of frequency, the noise subspace dimensionality reaches zero, and for any frequency higher than this the SD can only offer a performance equivalent to that of UD. In the current example, the dimension of the noise subspace of the SD becomes zero when the signal frequency exceeds 398 Hz, and at this frequency the SD method for case (a) becomes equivalent to the UD method because it uses all modes of the signal for detection, whereas the SD method for case (b) can no longer detect the signal as it has no information regarding the noise. The SD cannot be used when the frequency of the signal exceeds 423 Hz (in the current example).

The discussion so far establishes that lack of knowledge of the noise variance leads to deterioration in performance of detection in the case when there is no secondary data available to estimate the noise. However, it is of interest to know whether availability of secondary data can arrest this deterioration. Figure 4 is similar to Fig. 2, except that five secondary data vectors (sdv) are assumed to be available in case the ASFD, TSFD, TSD and SD do not possess knowledge of σ^2. Hence the detectors can estimate the value of σ^2 from the

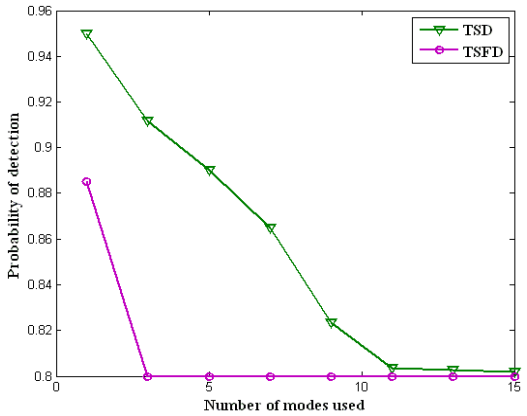

Fig. 6: P_D vs. number of signal modes T used for TSD and TSFD, SNR = -2 dB, f = 380 Hz, array geometry: HLA, source bearing: 33°

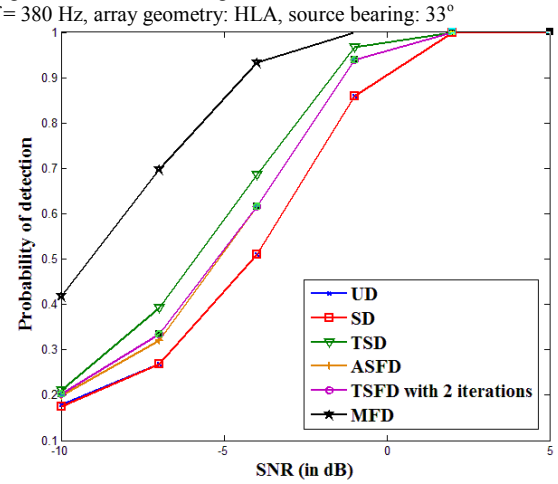

Fig. 7: P_D vs. SNR at P_{FA} = 0.1, f = 380 Hz, array geometry: HCA, source bearing: 33°

secondary data. It is seen that when sufficient sdv are available, all the detectors remain unaffected by lack of knowledge of σ^2.

The process of detection using any of the detectors (except the MFD) involves maximum likelihood estimation of the bearing angle ϕ, which is done by maximization of the test statistics with respect to ϕ. Hence the plot of variation of the test statistic over the scanned range of bearing angle of source acts as an ambiguity function of ϕ. The location of the peak of this ambiguity function provides an estimate of ϕ, and hence the peak of the detection test statistic acts as a rough bearing estimate of the source. Figure 5 shows the plots of normalized test statistics of the ASFD, TSFD and TSD, against the values of bearing angle ϕ scanned, when a source of frequency 380 Hz is detected at an *SNR* of -2 dB. The TSD is seen to provide the best estimate of ϕ among the three methods as it gives a sharp peak in the ambiguity function. The ambiguity functions of the ASFD and TSFD are seen to be almost coincidental.

In the results presented so far for horizontal arrays, the TSFD and TSD have been 'truncated' to use a single mode of the observed data vector for detection. It is of interest to observe the effect of using a higher number of modes on the performance of detection. Figure 6 shows the variation of the P_D when the number of modes used T is increased, when an HLA is used for detection. It may be observed that using

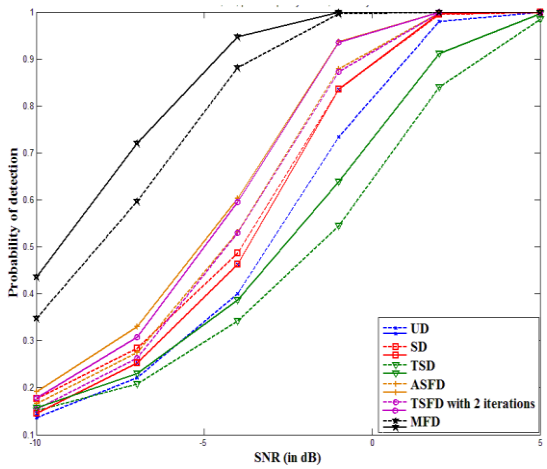

Fig. 8: P_D vs. SNR at P_{FA} = 0.1, f = 380 Hz, array geometry: VLA, source bearing: 33°, noise is considered to be spatially uncorrelated (solid line) and correlated (dashed line) between array elements.

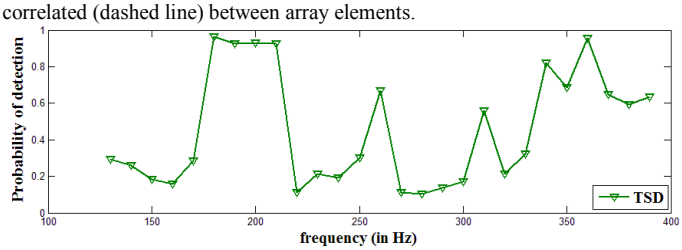

Fig. 9: P_D of TSD vs. frequency at P_{FA} = 0.1, SNR = -2 dB, array geometry: VLA, source bearing: 33°

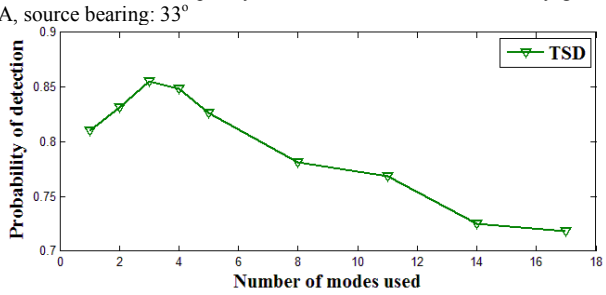

Fig. 10: P_D vs. number of signal modes T used for TSD at P_{FA} = 0.1, SNR = -2 dB, f = 380 Hz, array geometry: VLA, source bearing: 33°

higher number of modes clearly leads to degradation in the performance of detection. This may at first seem counter-intuitive, since using more information about the signal is expected to lead to better detection. However, the phenomenon can be explained for both the detectors as follows. In the case of the TSD, the degradation in performance as the number of modes used increases is due to the reduction in the noise subspace dimension [1]. Thus the degradation in performance due to reduction in information about noise is greater than the improvement in performance due to use of more signal modes. Hence the performance reduces. In the case of the TSFD, when $T > 2$, (47) and (48) become an under-determined system of equations. Hence the solution obtained by the minimum norm method is not accurate enough to improve the performance of detection. However if the number of used modes is only $T = 1$, the solution obtained is accurate, hence the P_D is higher.

The new detectors described in this paper can be readily adapted for use with a horizontal circular array (HCA) of AVS without any change in performance. This is demonstrated in Fig. 7 in which the variation of performance of detection of a

signal source by an HCA with variation in SNR is plotted for the same conditions as those in Fig. 2. Only detectors under case (a) are considered. A comparison of Fig. 2 and Fig. 7 shows that there is no considerable difference in performance when an HCA or HLA is used. Hence the proposed methods can be used for linear as well as circular arrays in the horizontal configuration.

When a vertical linear array (VLA) is used for detection, however, the performance of detection of all methods degrades in comparison to what is observed in the case of an HLA. This can be seen from Fig. 8, which shows the variation of P_D with the SNR when a VLA is used for detection (for case (a): σ^2 is known).Note that in this case the noise vectors at the elements of the sensor array may be correlated according to the covariance matrix in (18). In order to study the degradation due to spatial correlation, the performance is considered for two cases, namely when the noise at the elements of the array is considered to be spatially uncorrelated (solid line) and correlated (dashed line). All other experimental conditions for this figure are the same as for Fig. 2. It may be observed that in the case of all the methods except the TSD, the degradation in performance is marginal, and stems from the spatial correlation between the noise vectors. However, the TSD performs poorly when the array is used in the vertical configuration. This observation can be seen in detail from the plot of variation of P_D with frequency in Fig. 9. In this case the noise is considered to be spatially correlated according to (18). The plot shows that the performance of the TSD is highly fluctuating and deviates considerably from that observed in the case of HLA in Fig. 3. The poor performance of the TSD ($T = 1$) is due to the fact that the adverse impact of a drastic reduction in the number of modes on signal modeling is much higher in the case of a VLA. For each frequency, an optimal choice of T is necessary to attain the best performance of TSD using VLA. Figure 10 shows a plot of the P_D versus T for the TSD using a VLA, at the same experimental conditions as in Fig. 6. From Fig. 10, it may be seen that at the frequency $f = 380$ Hz, the performance of the TSD is optimal at $T = 3$. At this value of T, the TSD also outperforms the other methods. But the best value of T varies to some extent with the channel parameters and the signal frequency; the optimum value of T has to be determined numerically for the given conditions.

VI. Conclusion

This paper proposes three new schemes for signal detection using an array of acoustic vector sensors (AVS).The methods can be used for both horizontal and vertical arrays, and both linear and circular geometries. Two of the methods, namely the Approximate Signal Vector Form Detector (ASFD) and Truncated Signal Vector Form Detector (TSFD), require no prior information except the sound speed at the location of the sensors. These methods use the known relationship between the acoustic pressure and particle velocity components of the signal at each sensor, and are shown to outperform the conventional detection method called UD [1] at all frequencies of the signal. The TSD is a subspace detector, but it uses a truncated signal with T modes, where $T = 1$ for HLA and HCA and $T \sim 3$ for VLA. Hence TSD requires the knowledge of wavenumbers and mode functions of either the first mode only (for HLA and HCA) or the first few modes (for VLA), whereas the SD requires the wavenumbers and mode functions of all the modes. The performance of all the methods introduced in this paper is frequency-independent, and all of them are shown to outperform the SD [1] at higher frequencies of the signal or shorter array lengths. Their performance is also nearly optimal and close to that of the non-realizable matched filter detector. The computational complexity of these methods (particularly the ASFD) is much lower than that of the SD.

The performance of detection is found to degrade when the variance of environmental noise is not known. However, additional secondary data can be used to arrest this degradation. The performance also degrades when the noise at the elements of the sensor is spatially correlated in the case of a vertical array. For the horizontal arrays, TSD ($T = 1$) provides the best performance, followed by TSFD ($T = 1$). For the VLA, the TSD ($T = 1$) performs poorly, but its performance can be enhanced significantly by an optimal choice of T. All the proposed methods also provide rough estimates of the source bearing angle in the process of detection.

References

[1] K.M. Krishna and G.V. Anand, "Narrowband detection of acoustic source in shallow ocean using vector sensor array," *OCEANS 2009, MTS/IEEE Biloxi - Marine Technology for Our Future: Global and Local Challenges*, pp.1-8, 26-29 Oct. 2009

[2] A. Nehorai and E. Paldi, "Acoustic Vector-Sensor Array Processing," *IEEE Trans. Signal Processing*, vol. 42, no. 9, pp. 2481-2490, Sep. 1994

[3] K. G. Nagananda, G. V. Anand, "Subspace intersection method of high resolution bearing estimation in shallow ocean using acoustic vector sensors", *Signal Processing*, vol. 90, pp. 105 - 118, 2010

[4] G.L. D'Spain, W.S. Hodgkiss, G.L. Edmonds, "The simultaneous measurements of infrasonic acoustic particle velocity and acoustic pressure in the ocean by freely drifting swallow floats", *IEEE Journal of Oceanic Engineering* 16 (2) (April 1991) 195–207

[5] G.L. D'Spain, W.S. Hodgkiss, G.L. Edmonds, J.C. Nickles, F.H. Fisher, R.A. Hariss, "Initial analysis of the data from the vertical DIFAR array", *OCEANS '92. 'Mastering the Oceans Through Technology'. Proceedings.* , vol.1, no., pp.346-351, 26-29 Oct 1992

[6] S. M. Kay, *Fundamentals of Statistical Signal Processing, Vol.II: Detection Theory*. Upper Saddle River, New Jersey: Prentice-Hall, 1998.